



THERMAL ENERGY SCAVENGING To Power Aircraft Engine Test Sensors

A Major Qualifying Project Report:

Submitted to the Faculty of

WORCESTER POLYTECHNIC INSTITUTE

in partial fulfillment of the requirements for the

Degree of Bachelor of Science

by

Dustin Bradway

Daniel Bryand

Gregory Bukowski

Corina Scanio

April 18, 2008

Professor David J. Olinger, Advisor

Abstract

In order to validate the performance of their aircraft engines, Pratt & Whitney needs to measure pressures at various engine stations. Currently, the pressure transducers are powered by external power sources in a test stand. This setup requires the use of a great deal of wiring leading to long installation time and instrumentation system failures. The goal of this project was to power the pressure transducers wirelessly with a required 10 volt excitation at 10 milliamps. This was done by scavenging thermal energy from the engine with a thermoelectric generator package. This device uses the temperature difference between the engine exterior at station 12.5 and the surrounding ambient air to generate power. The generator was packaged between two metal plates with an attached heat sink to maximize the temperature difference and power output. Temperature differences of approximately 60 degrees Celsius and voltages of 2.5 volts were achieved for extended periods of time. A power converter was used to step up the voltage to the required 10V. In addition, rechargeable batteries were used to supplement the power during engine startup. This package will provide enough voltage to power most wireless devices and eliminate the problems associated with current instrumentation during engine tests at Pratt & Whitney.

Acknowledgements

We would like to thank the following people who supported the group throughout this process:

- Justin Urban and Kyle Vander Poel of Pratt & Whitney
- Professor David Olinger for his academic support and guidance
- Worcester Polytechnic Institute for the use of their resources

Table of Contents

Abstract.....	2
Acknowledgements.....	3
Table of Figures.....	5
List of Tables.....	6
1.0 Introduction.....	7
1.1 Project Objectives.....	8
2.0 Background.....	9
2.1 Vibrational Energy.....	9
2.2 Piezoelectrics.....	13
2.3 Thermal Energy.....	15
2.4 Fin Theory.....	18
3.0 Design Process.....	20
3.1 Clarification of Design Goals.....	20
3.1.1 Goals.....	20
3.2 . Generator Selection for Main Power Source.....	21
3.3 Design of Dual Power Electrical Circuit.....	21
3.4 Design of Thermal Plates.....	24
3.5 Heat Flow through Plates and Generator.....	25
4.0 Testing Procedure.....	30
4.1 Thermoelectric Device Testing.....	30
4.2 Velocity Measurement.....	33
4.3 Dual Power Supply Test Procedure.....	35
5.0 Results.....	39
5.1 Temperatures and Voltages Achieved.....	39
5.2 Power Results.....	41

5.3 Endurance Results.....	44
5.4 Heat Sink Optimization	45
6.0 Conclusion.....	52
6.1 Future Work.....	53
7.0 References	54

Table of Figures

Figure 1 - Model of a linear, inertial generator (Beeby, 2006)	10
Figure 2 - Compressive load and electrodes on the 3 axis (Boston Piezo-Optics Inc., 2008)	14
Figure 3 - Shear load on the 5 axis and electrodes on the 3 axis (Boston Piezo-Optics Inc., 2008)	14
Figure 4 - Performance graph of G1-1.4-219-1.14 model (Tellurex Corporation, 2007).....	17
Figure 5 - Finned Surfaces.....	18
Figure 6 - Schematic of Dual Power Circuit.....	22
Figure 7 - Schottky Diode	22
Figure 8: Schematic of Dual Power Circuit.....	23
Figure 9 - Schematic of Secondary/Primary Power Supply.....	24
Figure 10 - Plates and Generator	25
Figure 11 - Heat Flow	26
Figure 12 - a) Planned Temperature reading setup. b) Actual setup with Thermoelectric Generator and Thermistors.....	31
Figure 13 - Temperature Difference vs. Time (Noise).....	31
Figure 14 - Thermoelectric Generator between Plates with Heat Sink	33
Figure 15 - Velocity Test Design	34
Figure 16: Bottom Half of Circuit	35
Figure 17 - Test Circuit	36
Figure 18 - Power Supply and Digital Multimeter.....	37
Figure 19: Upper Half of Circuit	37

Figure 20: Temperatures, no wind.....	39
Figure 21: Temperatures, low speed wind (velocity 1m/s)	40
Figure 22: Voltage vs. Delta T	41
Figure 23: Power Test Set-up.....	41
Figure 24: Power vs. Temperature Difference.....	42
Figure 25 Power vs. Load Resistance	43
Figure 26: Aluminum Fin Heat Sink.....	45
Figure 27: Copper Fin Heat Sink.....	45
Figure 28: Temperatures using Copper Pin Heat Sink	46
Figure 29: Voltage using Copper Pin Heat Sink.....	46
Figure 30: Test Set Up	47
Figure 31: Temperatures using Long Aluminum Fin Heat Sink.....	47
Figure 32: Voltage using Long Aluminum Fin Heat Sink	48
Figure 33: Temperatures using Long Aluminum Fin Heat Sink with High Speed Fan	49
Figure 34: Voltage using Long Aluminum Fin Heat Sink with High Speed Fan	49
Figure 35 - Heat sink comparison	50
Figure 36 - Chosen heat sink for device	51
Figure 37: Final Thermoelectric Device Package	52

List of Tables

Table 1 - Energy Source vs. Performance (Beeby, 2006)	9
Table 2 - General Device Goals	21
Table 3 - Heat Transfer Conditions	26
Table 4 - Initial Conditions of Fin Calculation	28
Table 5 - Testing Results	33
Table 6 - Heat Sink Data.....	50

1.0 Introduction

In order for a jet engine to be installed on any airplane, it has to go through many tests to make sure that it will not fail under operating conditions. Some of the tests include validating the maximum thrust and checking various temperatures and pressures across the engine. One of the most important tests performed on the jet engine is to measure pressures and temperatures at different locations. To obtain pressure and temperature data, sensors, such as pressure transducers and thermocouples, are placed on the engine. With these sensors, the performance and efficiencies of the engine or specific components can be analyzed.

The sensors all require at least two wires. One wire is used to power the sensor and one is used to send the signal back to a data acquisition system. All the wires must be routed from each sensor, which considerably adds to test setup time and can become disorganized. The wires can take up too much space on the engine and instrumentation failures can occur.

To solve this problem, Pratt & Whitney, a main provider of jet engines for the world's aerospace industry, would like to implement a wireless system to monitor the engine. Currently engineers are studying wireless transmitters for sending the data back to the monitors. The problem of the wires is still not entirely eliminated since the sensors, and now the wireless transmitters, need power.

One solution is the use of batteries to power the wireless sensors. The problem is that batteries quickly deplete power resulting in frequent replacements. This is only useful when tests are short in time; however, Pratt & Whitney commonly runs test cycles that last for over 100 hours.

To eliminate all the wires, a feasible solution is to scavenge latent energy that the engine already produces. Jet engines create high temperatures in the burner section and have large spinning masses, which can cause vibrations. These energy sources can be tapped with an energy scavenging device placed on the exterior of the engine near the sensors. With small enough devices, the wires can be eliminated and each sensor can have its own power source and wireless transmitter.

This study will research existing methods of using energy scavenging methods to generate power from thermal and vibration sources. Size limitations of 3x3x3 inches and power requirements from ¼ - 3 Watts have been specified by J. Urban and K. VanderPoel of Pratt & Whitney. An energy scavenging system will be designed which meets the specifications including surviving the conditions found on the exterior of the engine while creating the required power.

1.1 Project Objectives

This project has three main objectives,

- Identify types of latent energy produced by a gas turbine operating in a test stand at Pratt & Whitney
- Design, build, and test a device to scavenge latent thermal energy produced by a gas turbine engine in order to power instrumentation
- Provide 10 V excitation to power pressure transducer instrumentation located on a gas turbine engine

2.0 Background

An understanding of energy scavenging methods was needed before a specific type was used for this project. The two forms of latent energy produced by a jet engine are vibrational and thermal. The theory of each method was researched and specific products were identified. The potential power levels of these products were compared and a final method was chosen to fit our constraints.

2.1 Vibrational Energy

Various energy scavenging techniques have been attempted and their power output has been tested and documented. Table 1 shows the types of energy sources which have been researched and developed by previous investigations, and their corresponding performance (Beeby, 2006).

Table 1 - Energy Source vs. Performance (Beeby, 2006)

Energy-harvesting opportunities and demonstrated capabilities.

Energy source	Performance ^A	Notes
Ambient radio frequency	< 1 $\mu\text{W}/\text{cm}^2$	Unless near a transmitter ³
Ambient light	100 mW/cm^2 (directed toward bright sun) 100 $\mu\text{W}/\text{cm}^2$ (illuminated office)	Common polycrystalline solar cells are 16%–17% efficient, while standard monocrystalline cells approach 20%. Although the numbers at left could vary widely with a given environment's light level, they're typical for the garden-variety solar cell Radio Shack sells (part 276-124).
Thermoelectric	60 $\mu\text{W}/\text{cm}^2$	Quoted for a Thermo Life generator at $\Delta T = 5^\circ\text{C}$ ⁸ ; typical thermoelectric generators $\leq 1\%$ efficient for $\Delta T < 40^\circ\text{C}$. ⁶
Vibrational microgenerators	4 $\mu\text{W}/\text{cm}^3$ (human motion—Hz) 800 $\mu\text{W}/\text{cm}^3$ (machines—kHz)	Predictions for 1 cm^3 generators. ⁹ Highly dependent on excitation (power tends to be proportional to ω^3 and y_0^2 , where ω is the driving frequency and y_0 is the input displacement), and larger structures can achieve higher power densities. The shake-driven flashlight of Figure 3, for example, delivers 2 mW/cm^3 at 3 Hz.
Ambient airflow	1 mW/cm^2	Demonstrated in microelectromechanical turbine at 30 liters/min. ²⁹
Push buttons	50 $\mu\text{J}/\text{N}$	Quoted at 3 V DC for the MIT Media Lab Device. ²⁰
Hand generators	30 W/kg	Quoted for Nissho Engineering's Tug Power (vs. 1.3 W/kg for a shake-driven flashlight). ²
Heel strike	7 W potentially available (1 cm deflection at 70 kg per 1 Hz walk)	Demonstrated systems: 800 mW with dielectric elastomer heel, ²⁶ 250–700 mW with hydraulic piezoelectric actuator shoes, ²⁴ 10 mW with piezoelectric insole. ²⁵

In the table the range of performance for any given energy source falls within $\mu\text{W} - \text{W}/\text{cm}^2$. This project requires a volume of 3x3x3 inches. Vibration energy produces approximately $\frac{1}{50}$ the amount of power of the $\frac{1}{4} - 3 \text{ W}$ range. The group researched two

possibilities from this chart, which could be effectively utilized with Pratt & Whitney’s aircraft engines. These two energy scavenging techniques were vibrational and thermal energy.

Vibration-powered generators are inertial-based systems which come in three types of vibration energy forms. These are piezoelectric, electromagnetic, and electrostatic. All three of these main transduction mechanisms are generally, but not always, inertial spring and mass systems. The maximum power generated within a resonant system is based upon a second-order spring and mass system most suited for electromagnetic power generation.

A model of a linear, inertial generator is shown in Figure 1. This includes a seismic mass m , attached to a spring with a stiffness coefficient k . Included in this inertial system are energy losses in the form of electrical energy, c_e , parasitic losses, c_p , which combine into the damping coefficient, c_T . When the inertial system is excited from an external source, the vibrations within the inertial system move out of phase in a sinusoidal expression. This behavior is represented by Equation 1.

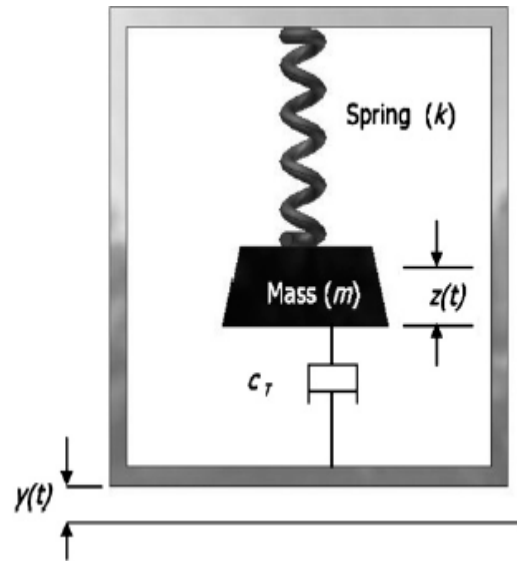


Figure 1 - Model of a linear, inertial generator (Beeby, 2006)

$$y(t)=Y\sin(\omega t) \tag{1}$$

Where Y is the amplitude, ω is the frequency, and t is time. This sinusoidal pattern moves out of phase with the external vibrations and creates a net displacement of the mass in the inertial system represented by $z(t)$ indicated in Figure 1 (Beeby, 2006).

The maximum power found within the inertial system is given by Equation 2.

$$P_e = \frac{m\zeta_e A^2}{4\omega_n(\zeta_p + \zeta_e)^2} \tag{2}$$

Where $A = \omega_n Y^2$ is the excitation acceleration levels and $\omega_n = \sqrt{k/m}$ is the natural frequency.

Maximum energy occurs when this natural frequency equals the excitation frequency. The equation $\zeta_p = c_p/(2m\omega_n)$ is the parasitic damping ratio and $\zeta_e = c_e/(2m\omega_n)$ is the electrical damping ratio. P_e is found to have a maximum value when $\zeta_p = \zeta_e$.

Electromagnetic theory is similar to that of a linear, inertial generator, however, it takes on a somewhat different form for its transduction damping coefficient. The damping coefficient, C_e , takes the form:

$$C_e = \frac{(NIB)^2}{R_{load} + R_{coil} + j\omega L_{coil}} \quad (3)$$

Where N is the number of turns around the coil, l is the side length of the coil, B is the flux density, R_{load} is the load resistance, R_{coil} is the coil resistance, L_{coil} is the coil inductance. Maximum power delivered to the system is shown in Equation 4 (Beeby, 2006).

$$R_{load} = R_{coil} + \frac{(NIB)^2}{C_p} \quad (4)$$

$$P_{e_{loadmax}} = \frac{mA^2}{16\zeta_p\omega_n} \left(1 - \frac{R_{coil}}{R_{load}}\right) \quad (5)$$

Electromagnetic induction was first discovered by physicist Michael Faraday in 1831, when he placed a conductor within a magnetic field, resulting in the generation of electrical current. The conductor took the form of a coil, while the electricity generated was the result of the relative motion between either a magnet and a coil, or changes within the magnetic field (Beeby, 2006). Today, the most promising way to scavenge energy from the environment using vibrations is by means of magnets, a coil and a resonant cantilever beam. In this practice, either the magnets or the coil should be fixed in place while the other creates a sinusoidal motion. Usually, the magnets are chosen to be fixed, acting as the inertial mass, and are passed through the magnetic field generated by the coil and cantilever beam. These experiments generate milliwatts of power as proven by past research.

One team of researchers led by Glynn-Jones experimented with using a coil wrapped around a cantilever beam, with two to four magnets fixed within the system. They first attempted two magnets to determine the output power with given amplitudes and frequencies, then the second prototype used four magnets with the same conditions (Beeby, 2006). The first prototype used a volume of 0.84 cm^3 and produced average power levels of $180 \text{ }\mu\text{W}$ with a displacement of approximately 0.85 mm (Beeby, 2006). These power levels were not sufficient for the team and four magnets were used with the hope to increase the output voltage and thus the power. To do this they needed to increase the magnetic coupling between the magnets and the coil. With the same conditions, including frequency of vibrations and amplitudes, the group nearly tripled the levels of output voltage to 1V rather than 300 mV . This resulted in approximately four times the output power the two magnet cantilever beam orientation produced.

Experiments for devices such as these require a simulation of typical conditions needed for vibration analysis. One common experimental practice is to use an engine block in a car. One can take a generator on a journey to determine both the instantaneous power levels as well as the average power generated. Glynn-Jones attempted this with his generator. He found that by taking his device mounted to an engine block on a 1.24 km journey, the instantaneous power level reached 4 mW and the overall average power was found to be $157 \text{ }\mu\text{W}$ (Beeby, 2006).

Commercially available electromagnetic generating devices are available today from several companies. One of these is a Dutch manufacturer, Kinetron, which both patents and produces electromechanical devices. Common applications from the generators that Kinetron has developed include wristwatches that power themselves from human movement, as well as headlights attached to a bicycle. Applicable devices available from Kinetron include rotary devices which output powers from $110 - 140 \text{ mW}$. This value depends upon the rotational speed, the number of windings, the excitation voltage, the resistance, and the frequency of the motor.

Another company, Perpetuum Ltd, based out of England, is a producer of electromagnetic generators. These generators, output power lower than Kinetron's, reaching up to 5 mW at an acceleration of 0.1 m/s^2 . These generators are used in common practice for networking wireless sensors (Beeby, 2006). However, neither of these commercially available products generates the power needed for this project. In fact, vibration energy in general produces very small amounts of power relative to the power required for this project.

2.2 Piezoelectrics

A piezoelectric material is one that creates an electric voltage when a mechanical load is applied. This load will deform the material, causing a separation of charges in the molecules which creates an electrical potential. This effect can also be reversed. An electric potential applied to a piezoelectric material will cause a mechanical deformation.

The piezoelectric effect is found naturally in a few crystals. A common example is quartz, which is used in most clocks and timing devices as an oscillator. Some other crystals include tourmaline, berlinite, and gallium orthophosphate. Ceramics like barium titanate and lead zirconate titanate and even some plastics also exhibit a piezoelectric effect, but are not found in nature (Piezo Systems, Inc., 2008).

Because the molecules in a piezoelectric material are polarized in a specific direction, loads in different directions on the same block will cause unique electric potentials. The same is true with the placement of the electric leads. The piezoelectric axes are denoted by 1, 2, and 3 where 3 is the polarization axis. An extra axis 5 is added for the application of a shear load. These polarization directions are created at the factory by exposing the crystal or ceramic to a large electric field.

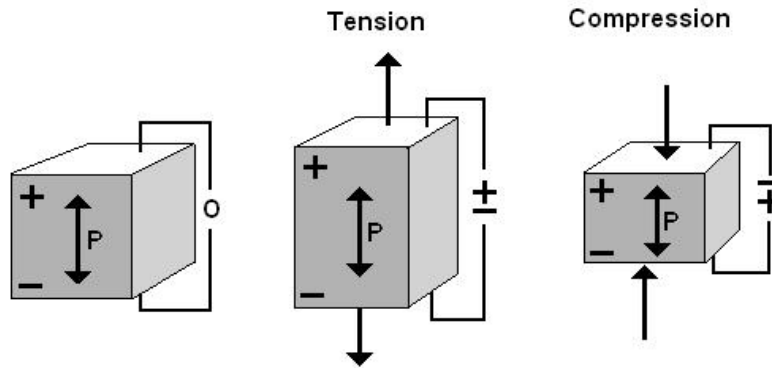


Figure 2 - Compressive load and electrodes on the 3 axis (Boston Piezo-Optics Inc., 2008)

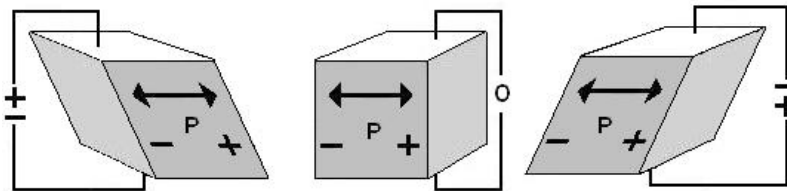


Figure 3 - Shear load on the 5 axis and electrodes on the 3 axis (Boston Piezo-Optics Inc., 2008)

Some important properties that define the characteristics of a piezoelectric material are the ratio of the voltage to mechanical strain “ d ”, or the strain constant, and the Curie temperature. The strain constant has units of meters per volt and can be found by Equation 6.

$$d = \frac{\text{strain}}{\text{voltage}} \quad (6)$$

This is used to find the relationship between the actual physical movement and the voltage created or applied to the material. Each axis of a piezoelectric block has a different strain constant. For example, in Figure 3 the strain constant would be denoted by d_{33} and in Figure 4 it would be d_{35} .

The Curie temperature is the temperature where the crystal form begins to change and depolarize. This causes the material to lose its piezoelectric properties. Once this temperature has been reached, the material has to be polarized once more to again become a piezoelectric.

Piezo Systems is a company that produces many different kinds of piezoelectric products. Some of these are small precision actuators or bending sensors, energy harvesters, and other kinds of oscillators. Another company is Boston Piezo-Optics. They produce transducer crystals for radios, ultrasonic transducers, and ultrasonic focusing housings. There are many applications that piezoelectric materials are used for, and these companies are just a small example of what is possible.

Again, this type of generator would be dependent upon displacements due to vibrations. As with the previous vibrational generators, a piezoelectric generator will only generate millivolts at very small amperages. Because of the small power generation capabilities, this method was not used.

2.3 Thermal Energy

Thermoelectric devices convert temperature differences directly into electric voltage. This effect was discovered in 1821 when Thomas Johann Seebeck observed that a circuit constructed of two different metals whose junctions are held at different temperatures creates an electrical current. The thermal gradient produced creates the voltage. A simple application of this effect is the wristwatch that uses body heat to power itself. A basic equation that describes this thermoelectric effect is seen in Equation 7.

$$V = a(T_h - T_c) \tag{7}$$

Where V is the voltage created, T_h is the hot temperature, T_c is the cold temperature, and a is the Seebeck coefficient. Materials with a high Seebeck coefficient, that is with a high electrical conductivity and low thermal conductivity, are ideal for thermoelectric generation. In 1834, Jean Charles Athanase Peltier discovered the opposite effect such that when a current is run through two dissimilar metals a thermal gradient is formed and can act as a heater or a cooler.

The Navy is using thermoelectric generators to power wireless sensors used in health monitoring. They too want to eliminate the cost and unreliability of batteries and tethered wires. They are using the technology from Hi-Z whose bismuth-telluride based thermoelectric generators harvest their power from the temperature difference between the equipment's relatively hot surface and the cooler surrounding air. This application has been successfully implemented using the cold surface of the ship's hull and the warmer air, a ΔT of only 5°C. The device created, however, is too large of a system for their needs. Their goal was to produce a device within one cubic inch. Hi-Z is now using Quantum Well thermoelectric generators. Quantum Wells are nanostructured multilayer films. This promising technology not only considerably reduces the size of the system, but also increases the efficiency by a factor of four. Since the Quantum Well generators can be used at temperatures up to 800°C, they can be used in the high-temperature sections of the gas turbine such as the combustor, turbine, and nozzle. The bismuth-telluride generators can only be used up to 250°C. This certainly could be applied to aircraft engines as well.

With all of the research that is being completed in the field of thermoelectric generators there has been a wide variety of companies that are attempting to capture latent energy that is normally lost in the environment. A few of the larger companies that are involved in producing power generating modules are Tellurex and Supercool.

Tellurex, a company located in Traverse City, Michigan, specializes in producing thermoelectric generators. They have received multiple rewards for their research in the thermoelectric field. Tellurex produces both cooling modules for electrical components and power generation modules. These modules cost from 23 to 45 dollars per unit. The power generating modules can produce from 1.5 to 5.7 watts (Tellurex Corporation, 2007). For example their high performance module has a power output of 5.7 watts and can generate 4.8 volts at 1.2 amps, while only taking up approximately 2.1 inches per side (Tellurex Corporation, 2007). The performance graph located in Figure 4, allows one to estimate the range of power that it can produce when the hot side of the plate is 150°C and the cold side of the plate is 50°C.

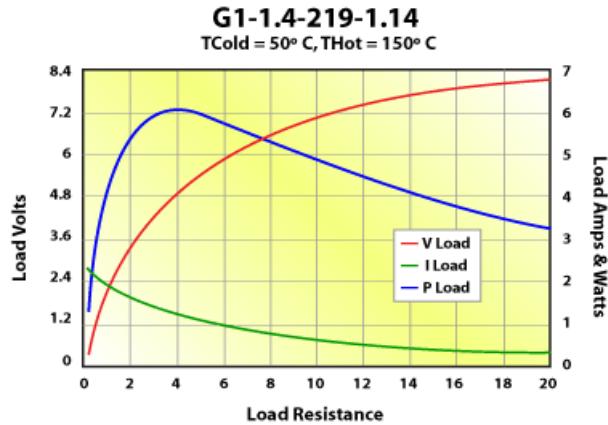


Figure 4 - Performance graph of G1-1.4-219-1.14 model (Tellurex Corporation, 2007)

Figure 4 is a great starting point to obtain an early estimate of power that is generated from one thermoelectric unit. The figure shows that the maximum values the thermoelectric generator can produce are around 6.1 Volts and 5.3Watts with a load resistance of 7.8 ohms.

Another company that produces thermoelectric power generators is Supercool, a unit of Laird Technologies. Supercool's main headquarters is in Sweden, but has a branch in California (Laird Technologies, 2007). Supercool has also received many awards for its research in the thermoelectric field. Supercool's goal is to produce thermoelectric modules whether it is a cooling or power module. They have a wide variety of designs for their power modules. These designs range from modules with a hole in the middle to modules that are similar to pyramids. The module that supplies the most power can operate at a maximum temperature of 120°C. The power modules that they produce can have a maximum power density of 14 watts per square centimeter (Laird Technologies, 2007). Supercool also produces and sells a wide variety of accessories, such as materials for insulation, and connectors for systems being built (Laird Technologies, 2007).

Because these thermoelectric generation methods produce more power than any vibrational energy scavenging devices, latent heat was chosen to power the sensors and wireless devices for this project.

2.4 Fin Theory

With the use of thermoelectric generators, enhancing the heat transfer from the surface is an important design consideration. Fins or extended surfaces from an object are common techniques for heat transfer enhancement. Along a fin the solid experiences heat transfer by conduction within its edges, as well as heat transfer by convection between its edges and the surrounding fluid (Naterer, 2003). Examples of different designs of finned surfaces are shown in Figure 5.



Figure 5 - Finned Surfaces

In one-dimensional fin analysis there are many general assumptions. The base temperature of the fin is assumed to be equal to the wall temperature of the main structure. The fin temperature is assumed to be one dimensional, meaning $T=T(x)$. The external heat transfer coefficient h_{∞} is assumed to be constant. Multi-dimensional analysis can be used but the one-dimensional idealization is quite adequate for design calculations. (Naterer, 2003) By applying an energy balance equation over a control volume yields Equation 8.

$$q_x'' A_c = q_x'' A_c + \frac{d}{dx}(q_x'' A_c) dx + (dA_s) h(T - T_{\infty}) \quad (8)$$

One can also derive an equation for the temperature and heat transfer of a uniform area fin:

Conditions: Tip convection

$$\text{Temperature: } \frac{T-T_{\infty}}{T_b-T_{\infty}} = \frac{\cosh(L/\lambda-x/\lambda)+Bi \sinh(L/\lambda-x/\lambda)}{\cosh(L/\lambda)+Bi \sinh(L/\lambda)} \quad (9)$$

$$\text{Heat Transfer: } \frac{q_b}{[(T_b-T_{\infty})(k_{\infty}PkA)]^{1/2}} = \frac{\sinh(L/\lambda)+Bi \cosh(L/\lambda)}{\cosh(L/\lambda)+Bi \sinh(L/\lambda)} \quad (10)$$

$$\lambda = \left(\frac{kA}{h_{\infty}P}\right)^{1/2} \quad Bi = \frac{h_{\infty}\lambda}{k} = \left(\frac{h_{\infty}A}{kP}\right)^{1/2} \quad (11)$$

An ideal fin would be perfectly conducting and would maintain an even surface temperature equal to its base temperature. Then its convection heat transfer would be a maximum. However, in an actual fin the temperature $t(x)$ decreases as x increases from the base (White, 1991). The efficiency of a fin can be defined as the ratio of the actual and the ideal heat transfer rate.

$$\eta = \frac{q_{actual}}{q_{ideal}} \quad (12)$$

One can then derive an efficiency equation for the fin convection condition.

$$\eta = \frac{\sinh(L/\lambda)+Bi \cosh(L/\lambda)}{\cosh(L/\lambda)+Bi \sinh(L/\lambda)} \left(\frac{\lambda}{L+A/P}\right) \quad (13)$$

Typically one would want an efficiency that is greater than 60%. Another quick way to determine if a design of a fin would be effective is if $\left(\frac{L+A/P}{\lambda}\right) \leq 1.5$ (White, 1991). Using these basic fin theory equations the project team can use fins to optimize the cooling of the “cool side” of the thermoelectric generator and in turn improve the efficiency of creating power.

3.0 Design Process

To create a device to electrically power pressure transducers a specific design process outlined in Dym and Little's (2004) textbook *Engineering Design: A Project-Based Introduction* was followed. This section details how the team went through the design process. First, a client interview was conducted with J. Urban and K. VanderPoel of Pratt and Whitney in order to obtain the information needed to develop a device. Then the group made a list of general device goals to reach. The team then made a design of a holding plate for the generator. Finally the team designed an electrical circuit to increase the power that will be delivered to the engine instruments.

3.1 Clarification of Design Goals

This section discusses the various design techniques that were utilized to generate a Revised Client Statement. To begin the process, the team identified the types of energy produced by a jet engine and how to harness this energy to produce power while keeping the device within the given constraints. With these attributes the team generated an organized outline of project requirements, as shown in Table 2.

3.1.1 Goals

The first step in the design process is to determine the requirements of the project. To address this step, the team interviewed with J. Urban and K. VanderPoel and developed a general list of the important requirements.

Table 2 - General Device Goals

Safety	Cannot harm Engine
	Cannot harm user
Cost	Should cost less than \$250
Mechanical Goals	Must adhere to device
	Must power Pressure Transducer
	Must withstand mechanical vibrations of X hz
User Friendly	Repeatability
	Minimal Training required
	Minimal Handling required
	Easy to use
Size	Smaller than 3x3x3 in
Power	At least 10 Volts at 10 milliamps
Placement	To be placed on exterior of gas turbine engine fan casing near station 12.5

3.2 . Generator Selection for Main Power Source

With the information gained in Table 2, the team was able to evaluate the different alternative design models. The team performed extensive brainstorming sessions within the team and with the client in order to consider all possible ideas.

A number of important factors had to be considered when selecting the final design. Not only did the design have to meet all objectives, functions and constraints, we also had to ensure that we utilized the time and resources available to us.

After a study of the vibrational and thermoelectric choices available, a thermoelectric power source was chosen. This type of generator gave us more power per square inch with a type of energy that is more readily available on a jet engine. The generator that was initially chosen for testing is the Tellurex G1-1.0-127-1.27. This unit was 1.3 x 1.2 inches and could output a max of 1.5 Watts. Later, the larger G1-1.4-219-1.14 unit was used with a foot print of 2.1 x 2.1 inches and a max output of 5.7 Watts.

3.3 Design of Dual Power Electrical Circuit

Thousands of sensors are required to relay information from the engine. Sensors require power to check system requirements such as temperatures and pressures across the engine in the early stages of engine start up. One of the problems to address within the system is how to power the wireless sensors prior to engine start up and after cool down. Currently, batteries

power the sensors. This becomes a problem when over time they need to be replaced. This is costly and time consuming.

A solution is to create a dual powered electrical circuit placed beside the generator. The circuit will feed power to the sensors prior to and during engine start up, allowing thermal differentials to build for the thermoelectric generator designed in this project to take effect. This allows a reliable power source to check invaluable information before the aircraft can fly. This dual powered electrical circuit will both provide power to the sensors and recharge a Polymer Li-Ion battery. A simple schematic of this circuit is shown in Figure 6.

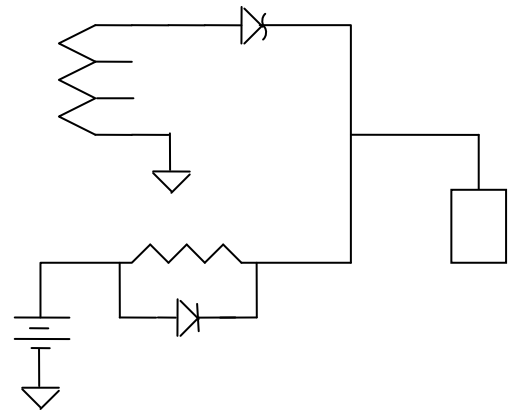


Figure 6 - Schematic of Dual Power Circuit

The circuit was designed to accomplish two functions. These were to power the required load before and after engine start-up. The first and most obvious solution was to create a rechargeable circuit. The constraints provided by the Pratt & Whitney supervisors for this project were that the load must have a 10 V excitation at 10 mA. Thus the circuit was designed around these constraints. There were two alternative considerations before the final circuit was implemented and tested. The first circuit had a string of diodes connected together in series from a power source to the load. This allowed for the voltage drop provided to the load be great enough as to allow the appropriate power required. However, a couple of problems with this design occurred. There is always some internal resistance within diodes, and with too many connected in series, the unknown variance in error was too great. Another disadvantage with this orientation was the space requirement for this circuit. Five to seven diodes would clutter the circuit too much for a 3 x 3 in circuit. The implemented design used Schottky diodes regulating the direction of current traveling into the load. Schottky diodes, shown in Figure 7, were selected because they are able to withstand a great deal of temperature before internal

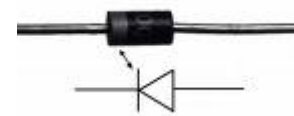
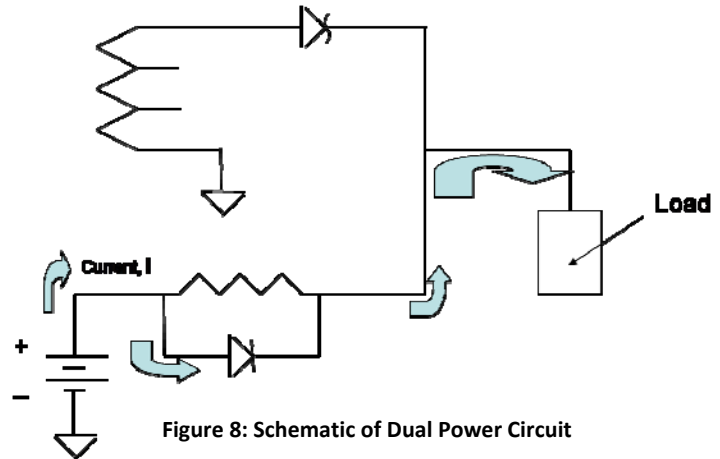


Figure 7 - Schottky Diode

breakdown and they have a small voltage drop.

The circuit accomplishes two tasks. First, it allows current to flow from the battery into the generator through a Schottky diode. This is accomplished by the lower half of the schematic shown in Figure 8. A fully charged

battery source of approximately 3.7 volts will send current at approximately 10 mA through the circuit (specification of Pratt & Whitney). The current travels through the circuit, then through a Schottky diode, approximately a 0.3 voltage drop (lowest voltage drop allowed by a diode). Then the current



passes through a resistor to moderate the amount going into the load where: $R = V/I$ where R represents electrical resistance, V represents voltage, and I represents current. The specifications provided by Pratt & Whitney require a 10 V excitation voltage at approximately 10 mA. Thus:

$$R = 10V/10mA = 1000 \Omega$$

By the time the current reaches the load, i.e. a wireless device, the voltage will be approximately 10 V, due to resulting voltage drops.

Once the output voltage is great enough from the generator, current is reversed in the circuit and the battery is recharged. A schematic of the circuit is shown in Figure 9 below. The top half of the circuit is a thermopile representing the thermoelectric generator. The engine will turn on and warm up creating heat generation. Once the thermal differential between the hot side and the cold side is great enough to generate over 10 V from the thermal generator, current will flow from the top half of the circuit down and into the load.

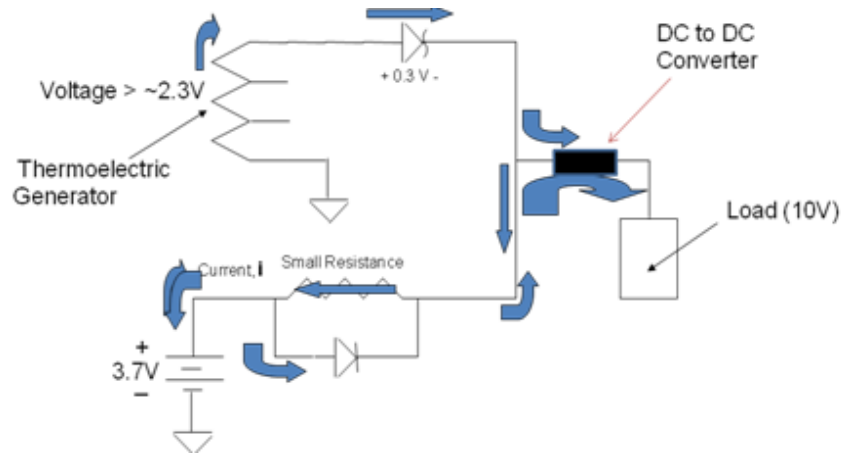


Figure 9 - Schematic of Secondary/Primary Power Supply

However, because the circuit is designed to be in parallel with the two power sources, current also flows back through the bottom half and into the rechargeable Polymer Li-Ion battery, thus recharging it.

3.4 Design of Thermal Plates

The generator created by Tellurex is made of two thin ceramic plates sandwiching hundreds of by-metal junctions. This design does not allow for the attachment of any heat sinks, temperature probes or support mechanisms. To solve this problem, a housing had to be created to hold the generator and all the support devices.

Some requirements for the plates include;

- Cavities for thermal probes on top and bottom
- Flat surface for heat sink attachment
- Large surface area for heat transfer

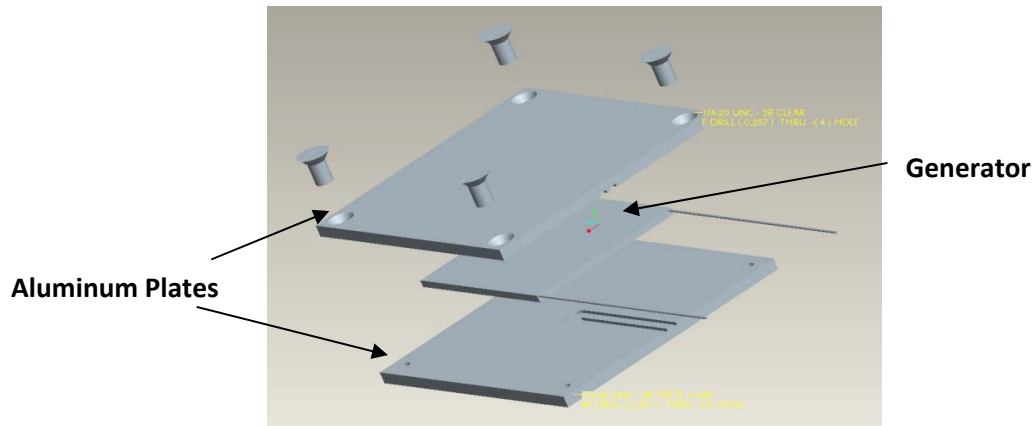


Figure 10 - Plates and Generator

The housing is two bolt together aluminum plates that sandwich the generator in between. In both halves, a pocket is cut to support the temperature probes. The top is counter-sunk to keep the bolts flush with the surface which gives a flat surface to mount heat sinks.

Instead of having the bolts held on with nuts from the other side, the bottom plate is threaded, and short bolts are used. This gives a flat surface on the bottom of the housing also to increase the conductive heat transfer.

3.5 Heat Flow through Plates and Generator

The following section outlines an initial heat flow problem for the heat flowing from the hot plate to the aluminum plate through the thermoelectric generator and finally through the aluminum plate to the ambient air. This heat flow is an example of conduction heat, which is the spontaneous transfer of thermal energy through matter, from a region of higher temperature to a region of lower temperature, and hence acts to even out temperature differences. The heat transfer problem is to calculate the heat transfer rate through the given setup and conditions in Table 3.

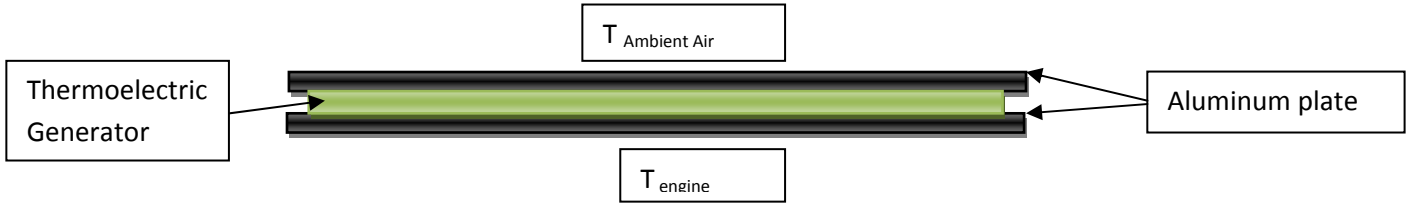


Figure 11 - Heat Flow

Table 3 - Heat Transfer Conditions

Material	Thermal Conductivity (W/mK)	Thickness (m)	Area (m ²)
Aluminum	237	0.006	0.0036
Ceramic Plates	2	0.000032	0.0036
Generator (Bismuth-Telluride)	1.20	0.0032	0.0036
Temperatures			
T _{Hot Plate}	180 C	453 K	
T _{Ambient Air}	23 C	296 K	

*measurements taken from Tellurex Specs Sheet and design of aluminum plates

Given these initial conditions and the type of heat transfer (conduction) Equation 14 is needed to calculate the heat flow through the setup in Figure 11.

$$\dot{Q} = \frac{1}{\sum_{i=1}^n \frac{\delta_i}{k_i}} A \times \Delta T \quad (14)$$

Where δ = thickness of material, k =thermal conductivity of material, A = Area of material

$$\dot{Q} = \frac{1}{\frac{\delta_{Aluminum}}{k_{Aluminum}} + \frac{\delta_{Ceramic\ Plates}}{k_{Ceramic\ Plates}} + \frac{\delta_{Generator}}{k_{Generator}} + \frac{\delta_{Ceramic\ Plates}}{k_{Ceramic\ Plates}} + \frac{\delta_{Aluminum}}{k_{Aluminum}} + \frac{\delta_{Air}}{k_{Air}}} A \times \Delta T \quad (15)$$

Plugging in the initial conditions

$$\dot{Q} = \frac{1}{\frac{0.006 \text{ m}}{237 \frac{\text{W}}{\text{mK}}} + \frac{0.000032 \text{ m}}{2.0 \frac{\text{W}}{\text{mK}}} + \frac{0.0032 \text{ m}}{1.20 \frac{\text{W}}{\text{mK}}} + \frac{0.000032 \text{ m}}{2.0 \frac{\text{W}}{\text{mK}}} + \frac{0.006 \text{ m}}{237 \frac{\text{W}}{\text{mK}}} + \frac{0.006 \text{ m}}{0.0261 \frac{\text{W}}{\text{mK}}}} 0.0036 \text{ m}^2 \times (453 - 296) \quad (16)$$

Completing the calculation yields $\dot{Q} = 2.426 \text{ W}$, this means that the device alone will not dissipate enough heat to cool off. With the addition of the heat sink the heat dissipation will increase even more.

If one looks at the temperature of the “cool-side” of the aluminum plate the following equation would be used

$$\dot{Q} = \frac{1}{\frac{\delta_{\text{Aluminum}}}{k_{\text{Aluminum}}} + \frac{\delta_{\text{Ceramic Plates}}}{k_{\text{Ceramic Plates}}} + \frac{\delta_{\text{Generator}}}{k_{\text{Generator}}} + \frac{\delta_{\text{Ceramic Plates}}}{k_{\text{Ceramic Plates}}} + \frac{\delta_{\text{Aluminum}}}{k_{\text{Aluminum}}}} A \times (T_{\text{Hot Plate}} - T_{\text{coolside}}) \quad (17)$$

The equation can be rearranged to solve for the temperature of the “cool side” of the aluminum plate

$$T_{\text{coolside}} = T_{\text{hot plate}} - \frac{Q \cdot \left(\frac{\delta_{\text{Aluminum}}}{k_{\text{Aluminum}}} + \frac{\delta_{\text{Ceramic Plates}}}{k_{\text{Ceramic Plates}}} + \frac{\delta_{\text{Generator}}}{k_{\text{Generator}}} + \frac{\delta_{\text{Ceramic Plates}}}{k_{\text{Ceramic Plates}}} + \frac{\delta_{\text{Aluminum}}}{k_{\text{Aluminum}}} \right)}{A} \quad (18)$$

Plugging in the numbers yields a temperature of 450.95K (177.95°C). This calculation shows that the cold side of the plate will reach a maximum temperature of 177.95 °C before it will start to cool off. The value of the temperature exceeds Tellurex’s specifications, which state that the cold side of the thermoelectric generator must not exceed a value of 125 °C. This calculation suggests that a heat sink will have to be added in order to increase the heat dissipation.

3.5.1 Heat Flow through Fins

The addition of a heat sink will increase the heat transfer from the top of the “cool side” to the ambient air. The theory of fins is described in detail in section 2.4. The calculation will take the convection of the heat sink into the ambient air. The heat flow will go from the base of the heat sink along the fins and convect into the air. The initial conditions are listed in Table 4.

Table 4 - Initial Conditions of Fin Calculation

Material	Thermal Conductivity (W/mK)	Thickness (m)	Length of fin (m)	Width of fin	Number of fins	Base Temperature (k)	Ambient Temperature (k)
Aluminum	237	4.3×10^{-4}	0.0509	0.0763	36	450	296

Equation 19 is needed in order to calculate the convection from the tip of a single fin. The first step is to calculate the efficiency of the fin using Equation 19.

$$\eta := \frac{\lambda}{Le + \frac{Ae}{P}} \cdot \left(\frac{\sinh\left(\frac{Le}{\lambda}\right) + B \cdot \cosh\left(\frac{Le}{\lambda}\right)}{B \cdot \sinh\left(\frac{Le}{\lambda}\right) + \cosh\left(\frac{Le}{\lambda}\right)} \right) \quad (19)$$

Where $\lambda := \left(\frac{k \cdot Ae}{h_{inf} \cdot P}\right)^{.5}$, $B := \left(\frac{h_{inf} \cdot Ae}{k \cdot P}\right)^{.5}$, Le is the length, Ae is the area, P is the perimeter.

Evaluating the equation yields an efficiency of 99.5%. This value is high due to the assumptions where the temperature is constant throughout the fin and does not change. However, this value is acceptable because the purpose of this calculation is to determine if a heat sink will increase the efficiency of our device. The next step is to calculate the ideal Q for a fin with having the assumption that 100% of the heat is dissipated. Equation 20 is then needed.

$$Q_{ideal} = h_{\infty}(T_{base} - T_{\infty})(P * L + A) \quad (20)$$

Plugging the numbers into the equation yields a Q of 0.334W per fin. To calculate the actual Q, the ideal Q needs to be multiplied by the efficiency factor. This yields a Q of 0.332W per fin. For this example there are 32 fins on this heat sink. So by multiplying the actual Q by the number of fins will give the total Q for the heat sink. This value is 10.631W. To ensure that it is a good idea to use a heat sink one must compare the difference and see if there is a sufficient change.

$$\frac{Q_{fin\ total}}{Q_{no\ fin}} = \frac{10.631}{2.426} = 4.382$$

By adding a heat sink it will transfer a little more than 4 times the heat than the base when there is no heat sink. This value verifies that adding a heat sink will increase the heat transfer rate and it will also increase the delta T by making sure the “cool side” stays cool.

4.0 Testing Procedure

The chosen approach to test the generator can be broken up into three parts:

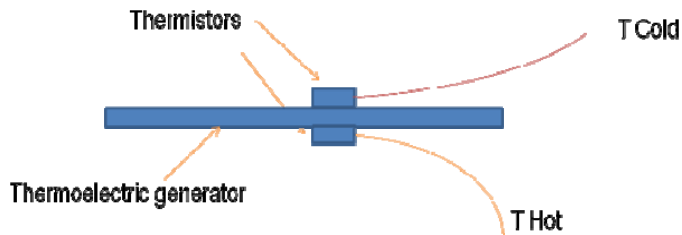
- 1) Measuring the voltage output
- 2) Measuring the temperature differences across the thermoelectric generator
- 3) Testing and determining the wind velocity across the generator and heat sink

All of these tests will contribute to the final design and optimization of the thermoelectric power generator.

4.1 Thermoelectric Device Testing

Initial testing of the thermoelectric generator consisted of connecting the generator leads to a voltmeter while holding the generator slightly above a hotplate. The hot side of the generator faced the hotplate, while the cool side of the generator was subjected only to the ambient air. The temperature difference between the hot and cold sides of the generator produced a voltage that was confirmed by the voltmeter. However, this testing only gives data on the voltage produced by the generator. The actual temperatures of the hot and cold sides of the generator were needed to be determined.

In order to test which temperature differences are producing which voltage output, a system was devised to measure the temperatures on both sides of the generator. Initially, a thermistor was simply taped on each side of the generator. The thermistors and the generator leads were connected to a data acquisition system controlled by LabView, as seen in Figure 12. A program was written that was able to read the temperature on each side of the generator as well as the voltage produced. This provided an easy way to compare the temperature difference and the corresponding voltage output.



a)



b)

Figure 12 - a) Planned Temperature reading setup. b) Actual setup with Thermoelectric Generator and Thermistors

However, the temperature readings that were produced contained a lot of noise which created inconsistent data, as seen in Figure 13. In effort to reduce that noise, thermal compound was added between the thermistors and the generator to strengthen the connection between them. In addition, an aluminum plate for the top and bottom of the generator were machined to keep this entire system together. The design and manufacture of these plates is discussed in Section 3.4.

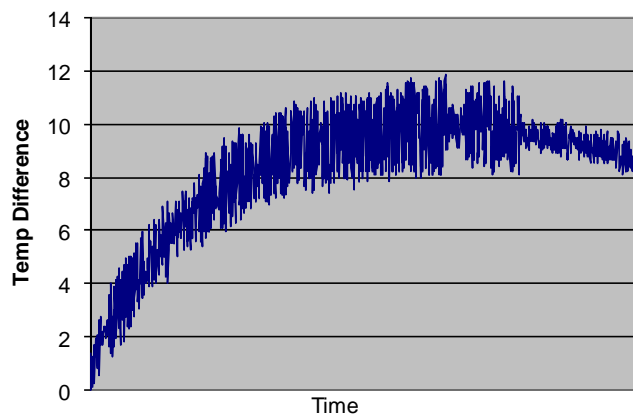


Figure 13 - Temperature Difference vs. Time (Noise)

With these changes added, the device was then tested again with the hotplate and the data acquisition system. The noise observed in the temperature readings was slightly reduced.

However, because of the aluminum plates, the temperature of the cold side of the generator was reaching close to its failure temperature. To make the cold side cooler, a fan was placed next to the hotplate to blow air over the cool side of the generator. This created slightly lower temperatures on the cold side. (Fan speed measurements can be seen in Section 4.2.)

The thermistors were replaced with thermocouples. The thermocouples not only gave more accurate readings, but also greatly reduced the amount of wires used in the system. While testing the device with the thermocouples, it was observed that when the hotplate was turned off, the noise in the temperature readings diminished. The noise also decreased when the device was taken off the hotplate. From this, it was determined that the hotplate itself was creating some noise, and direct contact with the hotplate is creating additional noise as well. To continue testing with the hotplate, the hotplate was heated up to its maximum temperature of about 200°C and then turned off. The device was placed on the hotplate, and the fan was turned on at its low setting. The measurements were then taken as the hotplate was cooling down.

With more accurate and consistent temperature readings, a heat sink was added to the cold side of the device. The procedure was repeated with the fan on low speed. As seen in Table 5 - Testing Results below, the temperature differences recorded with the heat sink were approximately 2°C higher than without the heat sink. Next, was to add thermal compound between the heat sink and the top of the device. The procedure was again repeated. The temperature differences then were approximately 5 °C higher than the heat sink results without the thermal compound. This confirmed the heat sink with thermal compound would be beneficial to this device.

Table 5 - Testing Results

<u>Low Fan Speed Testing</u>	<u>Temperature Difference</u>
Generator with plates	~10 °C
Heat sink added	~12 °C
Thermal paste added	~17 °C

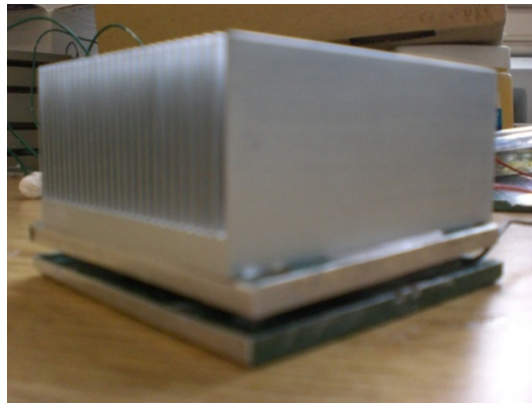


Figure 14 - Thermoelectric Generator between Plates with Heat Sink

Further testing included placing a piece of Sil-Pad 2000 placed between the device and the hot plate. This material made by Bergquist is a very good heat conductor and a poor electrical conductor. This material will be used in hopes that it will insulate the noise created by the hotplate. However, this pad did not diminish the noise. The next option was to ground the thermoelectric generator. This considerably reduced the noise. Grounding was then used in all further hotplate testing.

4.2 Velocity Measurement

The natural environment of the engine that the device will face in station 12.5 will include ambient wind velocities produced by the engine operating in a closed test cell. These wind velocities are very helpful because they will help with cooling the device. To simulate the

same environment that our device will encounter in the test cells, a velocity measurement test is needed to be conducted in order to determine ways to replicate the engine test environment. In order to measure the velocities one must have the following materials and set up:

- 1 digital manometer
- 1 Pitot static tube
- 1 fan
- 1 Ruler

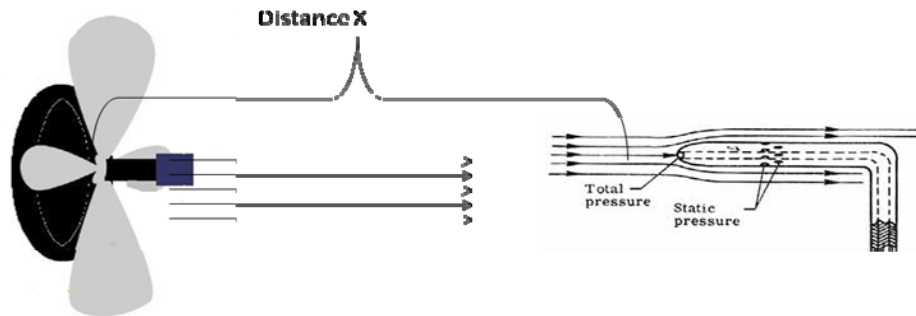


Figure 15 - Velocity Test Design

1. Attach the digital manometer kit tubes in to the appropriate locations
2. Measure out 10 cm from the base of the fan
3. Place pitot static tube on a sturdy surface so that it will not move
4. Turn on the digital manometer and the fan to high
5. Wait 30 seconds for fan to produce a steady velocity
6. Record digital reading, the number that is recorded is the amount of inches of water that is displaced the Δh
7. Repeat steps 3-6 for the following distances 15cm, 20cm, 25cm, 30cm.
8. Repeat steps 2-7 for the low speed setting on the fan

When completed with recording the data from the digital monometer use Equation 21 to calculate the velocity:

$$V = \sqrt{\frac{2\rho_{h_2o}gh}{\rho_{air}}} \quad (21)$$

Where

V – velocity

ρ_{h_2o} – density of water

g – gravity

h – measurement off of digital monometer

ρ_{air} – density of water

4.3 Dual Power Supply Test Procedure

The circuit was tested using a breadboard. The represented load was substituted with a 3 V green LED, the thermoelectric generator was substituted by an actual power supply, and three 1.2 V NiMH rechargeable batteries were used. First the bottom half of the circuit, shown in Figure 16, was constructed on the breadboard. When the circuit was closed, the design was confirmed by lighting a green LED.

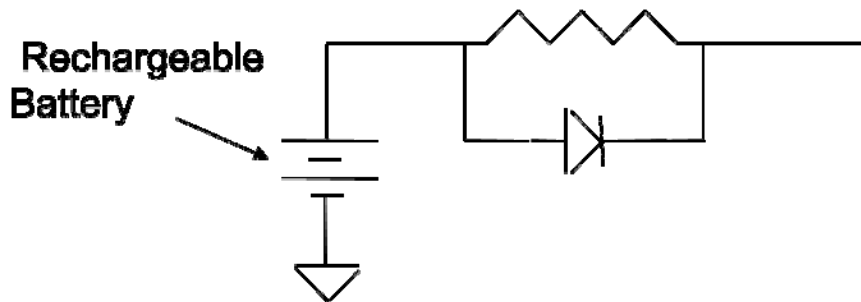


Figure 16: Bottom Half of Circuit

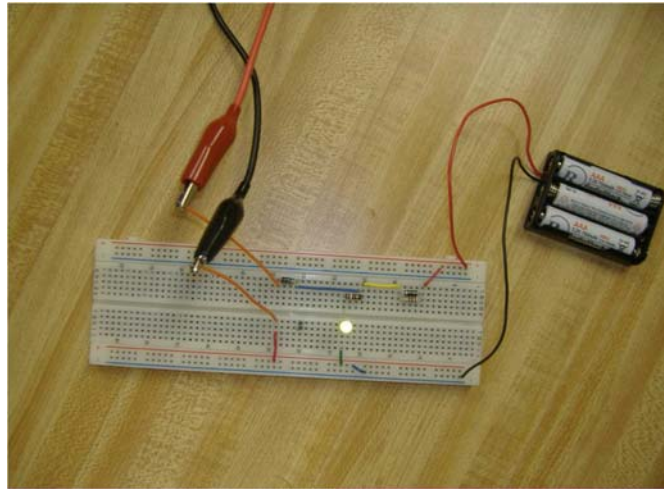


Figure 17 - Test Circuit

Using a Digital Multi-Meter (DMM) it was shown that the voltage was slowly decreasing.

Steps to determine circuit voltages:

1. Hook the positive and negative leads (representing the generator) up to the power supply. Make sure to keep the power supply off.
2. Attach the positive and negative leads of the DMM to either side of the LED.
3. Verify the voltage drop across the load is approximately equal to the battery voltage.
4. Turn the power supply on. Increasing the voltage to two different voltages. The first to approximately 1 V below the previous voltage reading. Second, to a voltage approximately 1 V above the previous reading.
5. Verify that the voltage read on the DMM changes from decreasing to increasing voltage according to step 4, respectively.

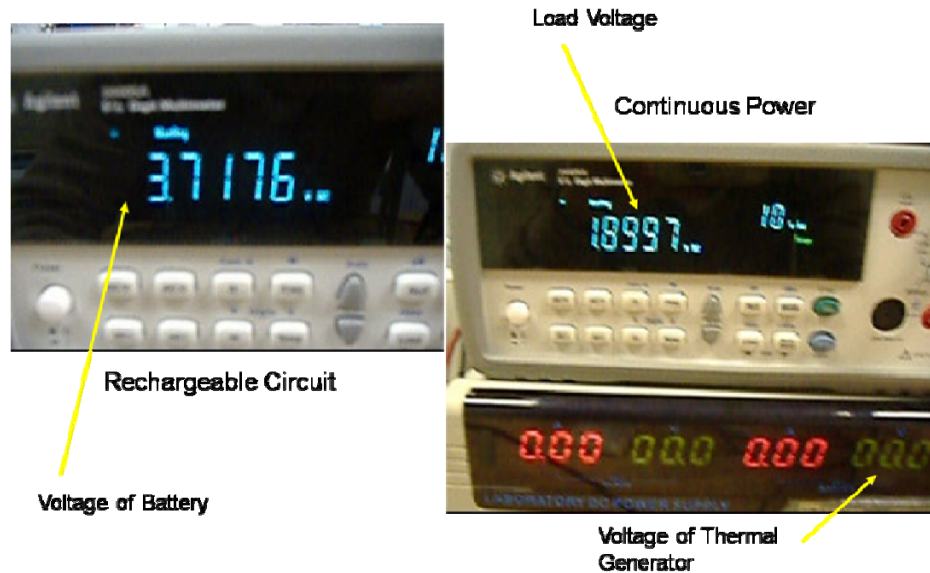


Figure 18 - Power Supply and Digital Multimeter

Next, the upper half of the circuit, shown in Figure 19 was constructed on the protoboard.

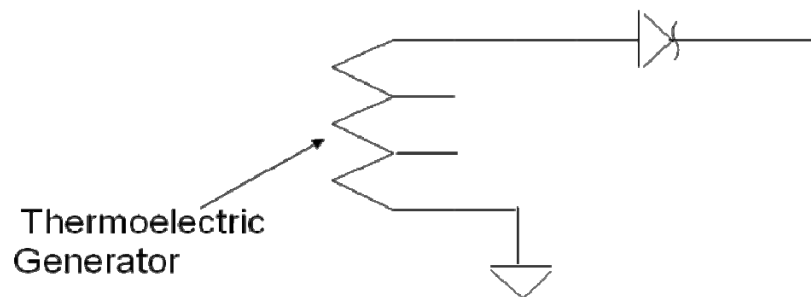


Figure 19: Upper Half of Circuit

The most important thing with the circuit is to make sure power is supplied to the load. Therefore, the first half of the circuit was disconnected and only the thermoelectric generator (power supply) was connected. By increasing the voltage from 0-3 volts the LED illuminated brighter and brighter indicating that the power was increasing with increased voltage. Once this was confirmed, the concept of a rechargeable circuit was demonstrated. With both the battery and power supply connected the battery was first powering the LED. Then, doing a simple demonstration of the power supply increasing voltage from 0 to 3+ volts (as the actual generator would do) the current was reversed. The DMM showed the voltage increase once the

power supply voltage exceeded the battery voltage. This proved the theory that the circuit was rechargeable and practical.

5.0 Results

5.1 Temperatures and Voltages Achieved

Once the noise problem was solved with grounding the hotplate, more accurate testing could be performed. First, the temperature difference across the thermoelectric generator was measured again to determine the greatest achievable change in temperature across the generator with the temperatures produced by the hotplate. A thermocouple was placed on both the hot side and on the cold side of the generator which measured the temperature of the respective sides. The thermocouples were then connected to the LabView data acquisition system. The entire device with the aluminum plates and a heat sink was placed on the hotplate. As the hotplate heated up, the change in temperature could be seen increasing on the LabView graph. Figure 20 shows the temperature of the hotplate compared to the temperatures of the hot and cold side of the generator. As the hotplate heats up, the temperature on the hot side of the generator is also seen to increase. The temperature on the cold side also increases but not as rapidly as the hot side. This difference in the rate of temperature escalation causes the change in temperature across the generator to increase. Figure 21 shows the hot side and cold side temperature lines getting further apart. A change in temperature of 40.63°C was achieved at a hotplate temperature of 98.16°C .

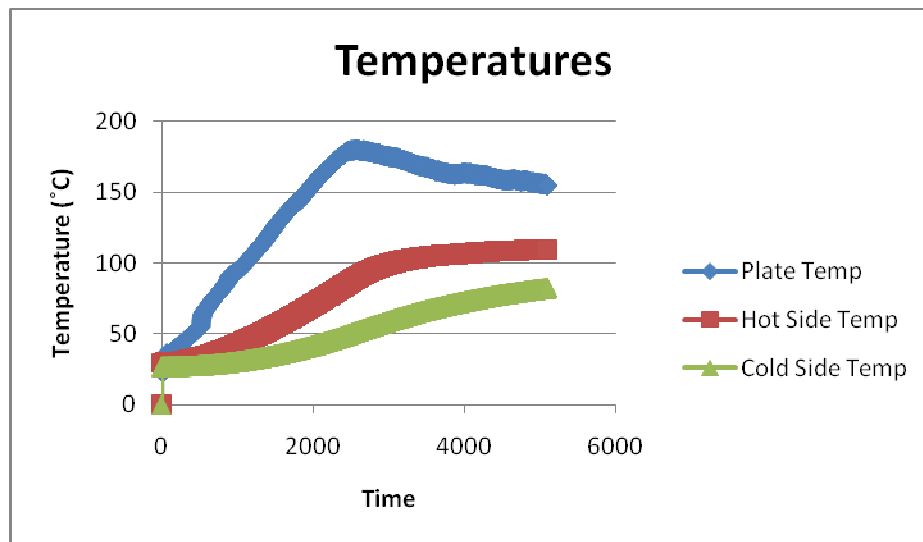


Figure 20: Temperatures, no wind

Then a fan was placed 14.5cm from the hotplate and blew air over the device on its low setting. The fan allowed for a 2°C increase in the change in temperature by keeping the cold side cooler.

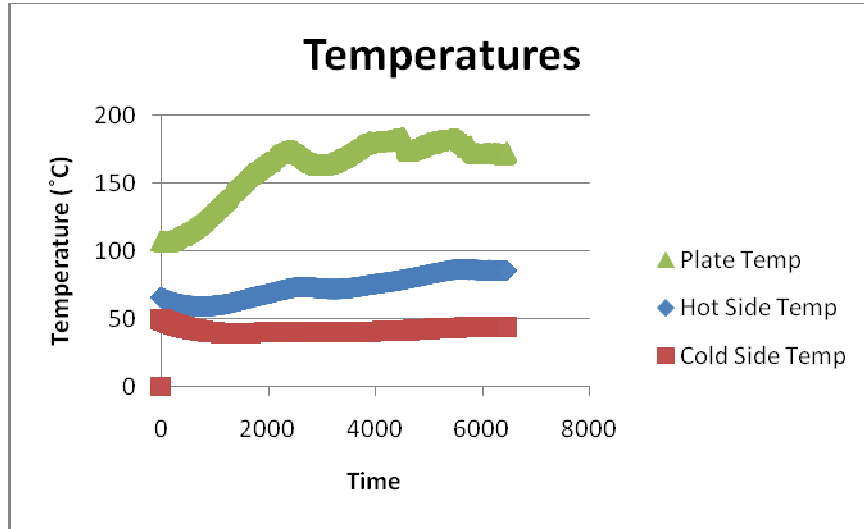


Figure 21: Temperatures, low speed wind (velocity 1m/s)

The voltages were read off a voltmeter and updated in LabView. As the change in temperature increases, the voltage produced also increases as shown in Figure 22. The voltage vs. temperature change is precisely linear. With a hotplate temperature of 86.11 °C, a change in temperature across the generator of 42.34 °C was achieved. That change in temperature produced a voltage of 2.13V.

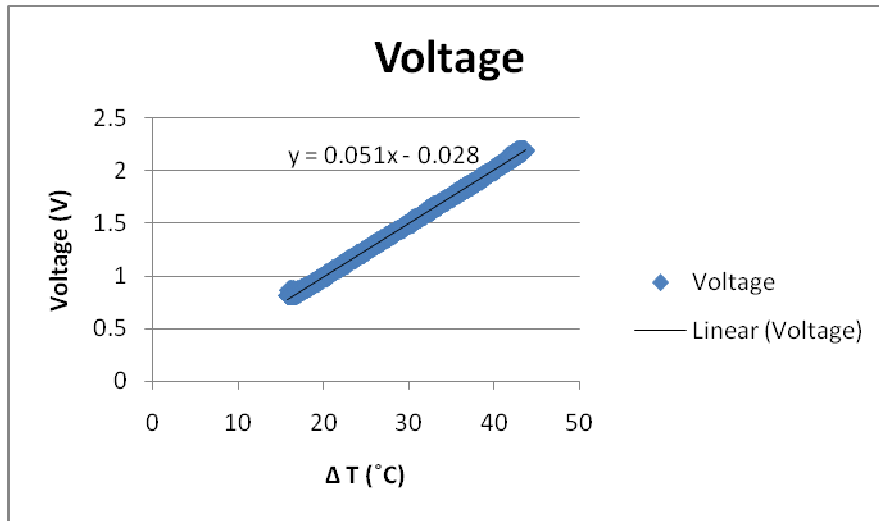


Figure 22: Voltage vs. Delta T

5.2 Power Results

Pratt and Whitney is looking to power as many devices on a test engine as possible. The thermoelectric generator must create as much amperage as possible at the steady 10 volts for the pressure transducers.

The Tellurex generator's specifications state that the max power generation for the large model is 5.7 watts. The power output is dependent upon both the temperature difference across the ceramic plates and the resistive load placed on the generator output.

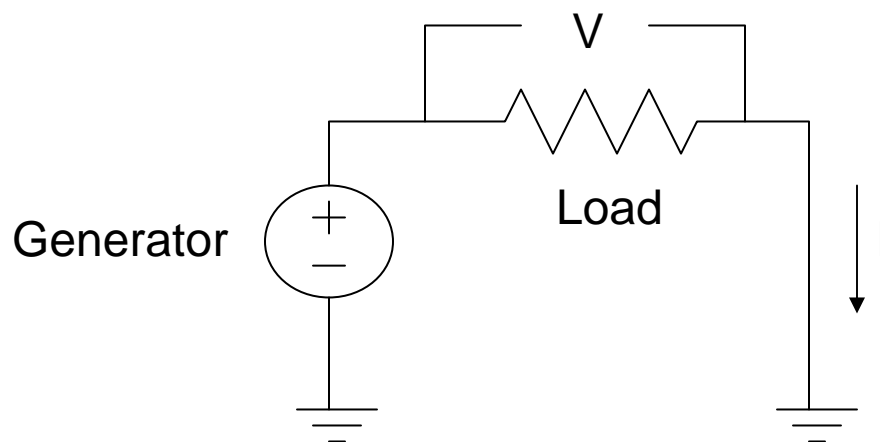


Figure 23: Power Test Set-up

A simple test was run on the generator alone with the setup shown in Figure 23. A 10kΩ resistor was added to the output of the generator. While the generator was allowed to cool, the voltage across and the current through the resistor was measured. With this information, the power was calculated by $P = I \cdot R$. The power verse temperature difference is shown in Figure 24.

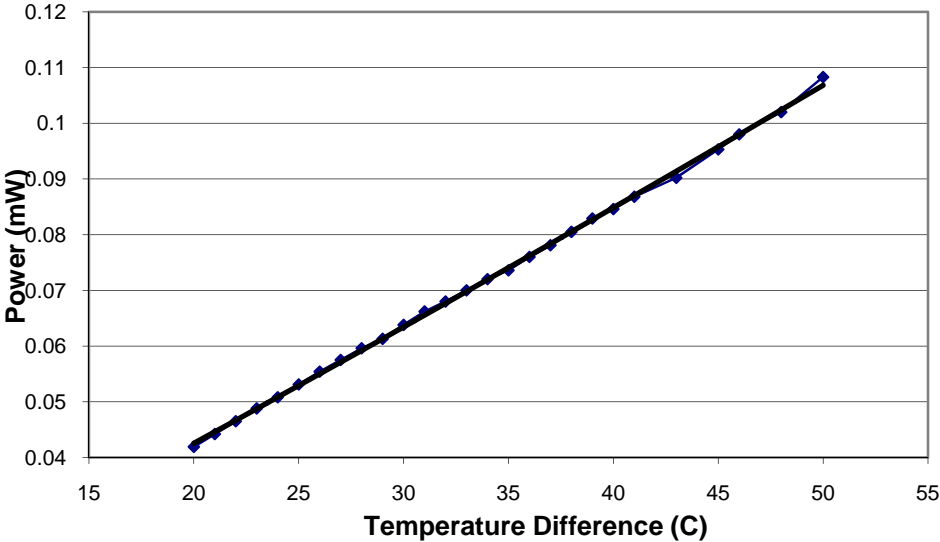


Figure 24: Power vs. Temperature Difference

Because of the large resistance used in this experiment, the power being dissipated was very low; slightly over .1 mW at a temperature difference of 50°C. With a lower resistive load, the current draw, and therefore, power output will be greater. An estimated power output at the maximum temperature difference of 100°C is shown in Figure 24.



Figure 25 Power vs. Load Resistance

Figure 25 shows the power generated after the 10 volt step up conversion. There is a loss of about 80% through the two step-up converters, which is taken into consideration.

The amount of power produced by the Tellurex G1-1.4-219-1.14 thermoelectric generator is more than enough to power multiple pressure transducers which require 10 volts and 10 mA each. This is only a power needed of $10\text{v} * .01\text{ A} = .1\text{ Watts}$ per transducer. With the generator running at about a 2.5 Watt output ($\sim 50^\circ\text{C}$ delta T), 25 pressure transducers can be supported.

5.3 Endurance Results

The group also considered the amount of time that components such as pressure transducers on the engine should be powered. Realistically, the aircraft will endure between 2-12 hours of flight time. This means the power generated from our device should continually run past this time span. The group ran an endurance test with the thermoelectric generator to ensure its endurance capability under specific operating conditions.

Using the procedure described in Section 5.1, the group performed a 24-hour endurance test. Pratt & Whitney specified that the operating conditions would include a temperature range between 50-150 °C and low to almost no internal wind speeds. The group kept these specifications in mind when performing the experiment. The group attempted to generate as much voltage as possible under the maximum operating temperature. Therefore, a steady state temperature range was chosen between 138-145 °C, with a delta T of 75-76 °C. This resulted in a voltage generation between 4.96-5.15 V. The wind speed was kept constant at 1 m/s (2.25 mph).

The group obtained important results from this experiment. During the first few hours of the experiment, two generators failed because they exceeded their maximum rated operating temperature. This was found to be 175 °C. Therefore, for the remainder of the experiment, the temperature was kept no higher than 150 °C. Also, we attempted to find the operating conditions with natural convection by turning the fan off from its original 1 m/s wind speed. This resulted in the cold side temperature of the heat sink to rapidly spike, which decreased our delta T and voltage values. Therefore, it was concluded that wind, even a small amount, was required for stable power generation.

5.4 Heat Sink Optimization

The three different heat sinks were tested to determine which design kept the cool side of the generator the coolest. The above tests used the aluminum fin heat sink design shown in Figure 26.



Figure 26: Aluminum Fin Heat Sink

Using the copper pin heat sink created a greater change in temperature. When the hotplate was at a temperature of 106.5°C , the change in temperature across the generator was 51.42°C . This produced a voltage of 2.68V. These results are in Figure 28 and Figure 29.

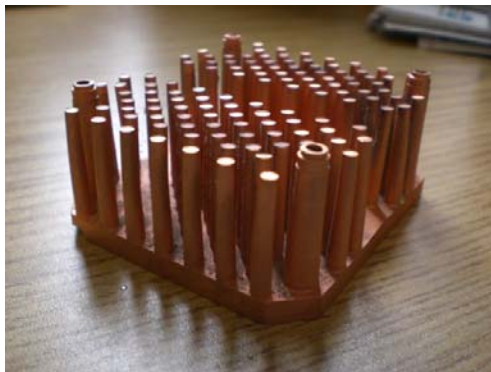


Figure 27: Copper Fin Heat Sink

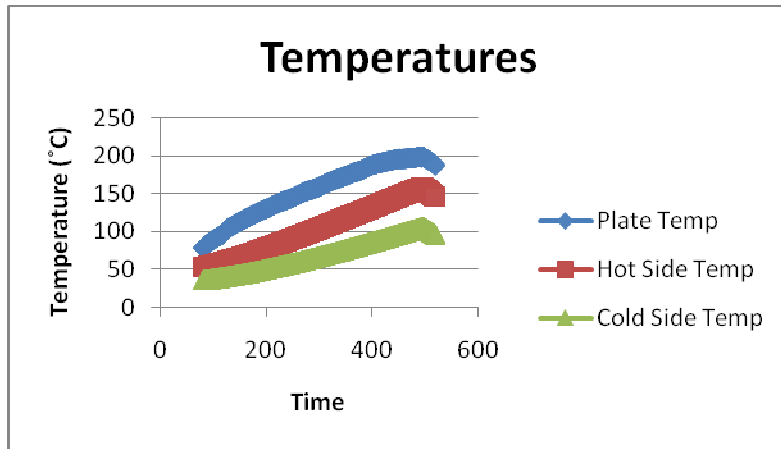


Figure 28: Temperatures using Copper Pin Heat Sink

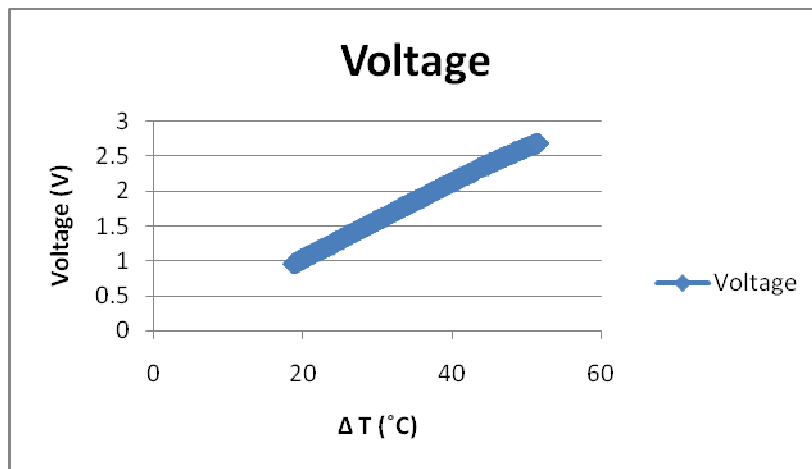


Figure 29: Voltage using Copper Pin Heat Sink

Another aluminum heat sink was used which has longer fins, as show in Figure 30. At a hotplate temperature of 127.8°C, a change in temperature of 49.71°C was achieved. This produced a voltage of 2.62V.



Figure 30: Test Set Up

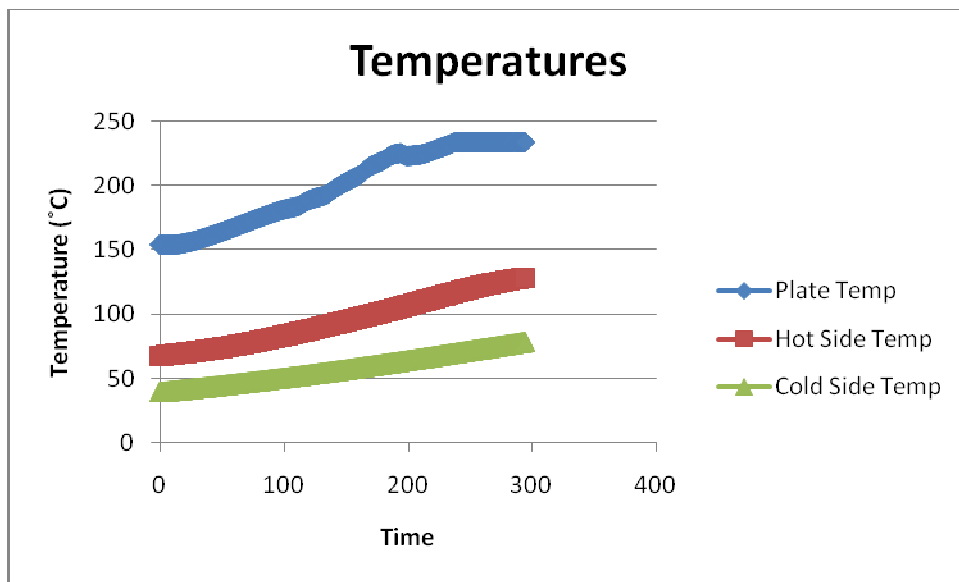


Figure 31: Temperatures using Long Aluminum Fin Heat Sink

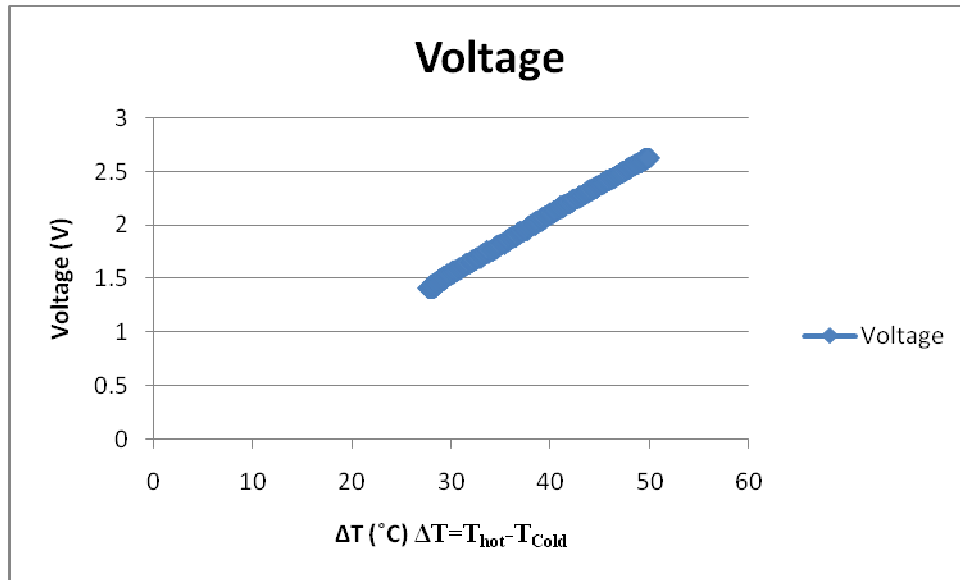


Figure 32: Voltage using Long Aluminum Fin Heat Sink

Using the same heat sink with the fan now on its high setting created a change in temperature of 54.65°C. That produced a voltage of 3.18V. The voltage regulator package was added at that time and the voltage jumped up to 5.56V, as seen in Figure 34. When the temperature difference reached 56.62 °C, a voltage of 5.72V was achieved. Because of the desirable results with this heat sink, it was decided to continue its use.

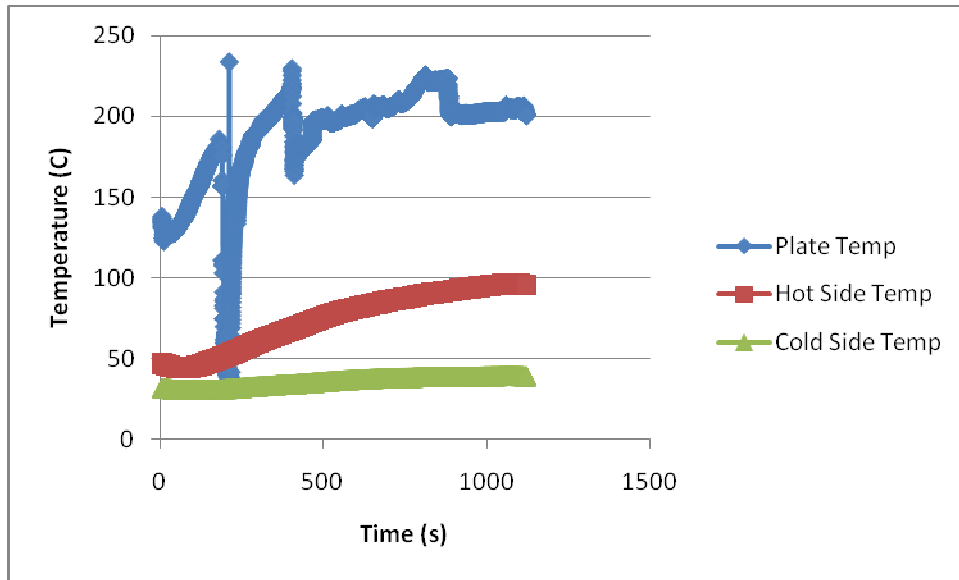


Figure 33: Temperatures using Long Aluminum Fin Heat Sink with High Speed Fan

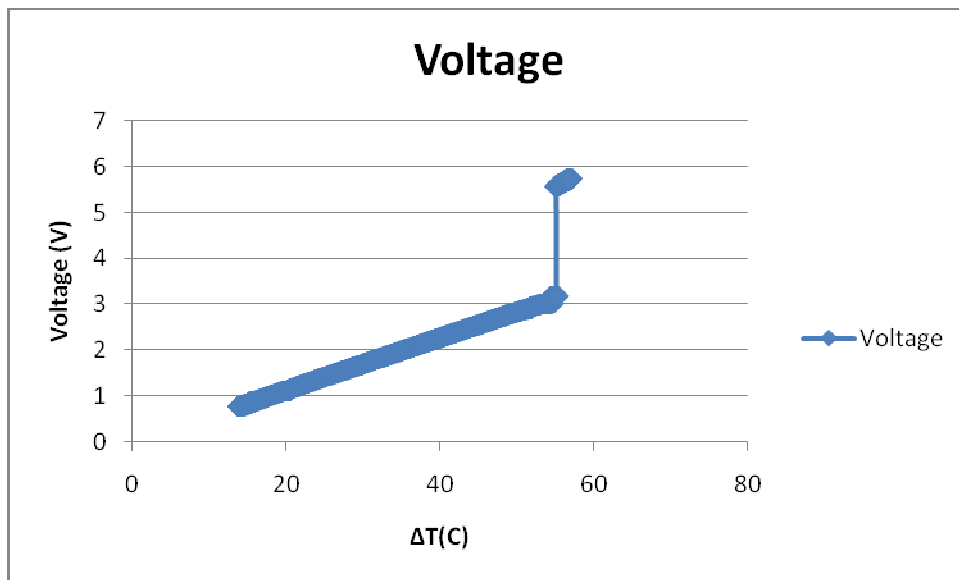


Figure 34: Voltage using Long Aluminum Fin Heat Sink with High Speed Fan

Table 6 and Figure 35 display all of the combined test data and information of the three heat sinks. This table allowed the team to easily look at the differences between the heat sinks and determine the best heat sink for our device.

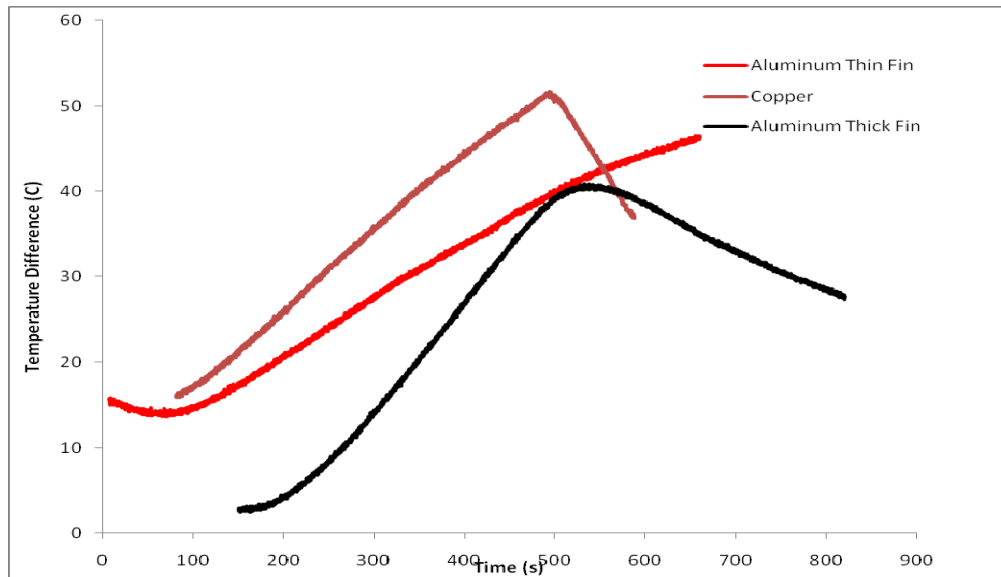


Figure 35 - Heat sink comparison

Table 6 - Heat Sink Data

Heat Sink	Copper	Aluminum short Thick Fin	Aluminum Tall thin fin
Type of Fin	Pole	Rectangle	Rectangle
Length of Fin (m)	0.0207	0.0302	0.0509
Width/Diameter (in)	0.0026	0.0832	0.0763
thickness	0.0026	9.50E-04	4.30E-04
Surface Area (m ²)	5E-05	0.00502528	0.00776734
Number of Fins	116	27	32
Total Fin area (m ²)	0.0062	0.13568256	0.24855488
Distance between fins (m)	0.0045	0.002	0.0016
Total Distance Between Fins (m)	0.522	0.054	0.0512
Delta T reached (C)	51.42	42.34	54.65
Voltage (v)	2.68	2.13	3.13
Q(W) per fin	0.085	0.219	0.332
Q(W) Total	9.806	5.926	10.631

Figure 35 shows the data that was collected from the three different heat sinks. The copper heat sink initially created the greatest delta T but after approximately 500 seconds it had reached its maximum and could not dissipate the heat faster than the cool side was heating up. The aluminum short thick fin had the same characteristics. However, the aluminum long

thin fin heat sink had a steady increasing delta T and a maximum delta T was never reached in this test. Table 6 clearly shows that the aluminum tall thin fin heat sink, shown in Figure 36, outperformed the other heat sinks.



Figure 36 - Chosen heat sink for device

6.0 Conclusion

The final deliverable of this project is an operating thermal energy scavenging device that uses the temperature difference between its two sides to generate a voltage, as shown in Figure 37. The performance of a Tellurex power generation model was improved with the use of aluminum plates and a heat sink. It is able to sit on a heated surface and produce 10 volts to power a small electric device. With a temperature difference of approximately 45 °C it is capable of producing 2.3 volts. The voltage is then amplified to 10 volts through two DC to DC converters. Its performance has been validated through many experimental tests. It is also operational during engine start up before the engine reaches operating temperatures. This is accomplished through a lithium ion battery which can then be recharged while the generator is running. In the presence of a low velocity ambient air flow of approximately 1 m/s, the device is able to run for extended periods of time, as demonstrated with a twenty-four hour endurance test. The device will be able to be placed on a small 3 in by 3 in area on the exterior of a gas turbine engine and use the temperature differential between the heat of the engine and the ambient air to power instrumentation. In this case, it could power many pressure transducers. The device is convenient because it will eliminate wiring that would have been necessary to power the sensors, thereby reducing setup time and contributing to the organization of the engine testing process.

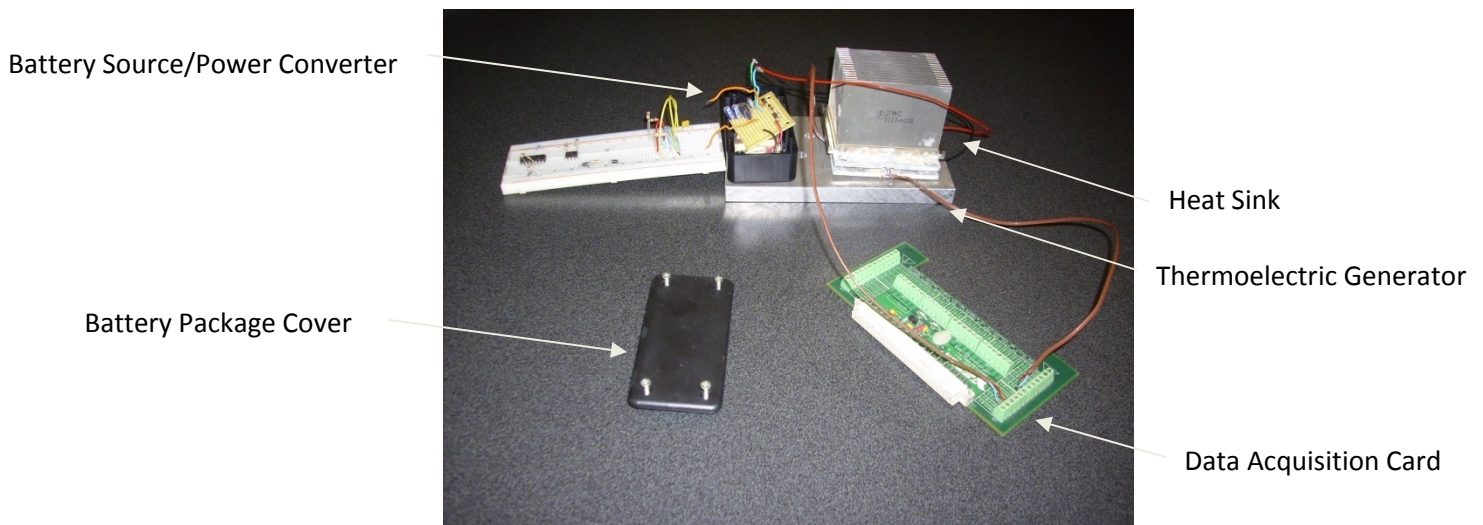


Figure 37: Final Thermoelectric Device Package

6.1 Future Work

- Complete engine test where thermoelectric device is placed on car engine
- Complete vibrational test with operating condition similar to that of a gas turbine engine
- Develop a package for the thermoelectric device
- Develop a more advanced battery management system
- Test the thermoelectric device on a gas turbine engine

7.0 References

1. Beeby, S.P., Tudor M.J., and White, N.M. "Energy Harvesting Vibration Sources for Microsystems Applications." *Measurement Science and Technology*. 2006.
2. White, Frank M., *Heat and Mass Transfer*, Addison-Wesley, Reading, MA, 1991.
3. "An Introduction to Piezoelectric Transducer Crystals," Boston Piezo-Optics, Inc., Bellingham MA. [<http://www.bostonpiezooptics.com>. Accessed 10/07.]
4. "An Introduction to Thermoelectrics," Tellurex Corporation, Traverse City MI, 2001. [<http://www.tellurex.com/cthermo.html>. Accessed 10/07.]
5. "Piezo Terminology," Piezo Systems, Inc., Cambridge MA, 2007. [<http://www.piezo.com/tech1terms.html>. Accessed 10/07.]